




Controlling spatial coherence with an optical complex medium: supplement

ALFONSO NARDI,^{1,*}  FELIX TEBBENJOHANN,^{1,2} MASSIMILIANO ROSSI,¹  SHAWN DIVITT,³  ANDREAS NORRMAN,^{1,4}  SYLVAIN GIGAN,⁵ MARTIN FRIMMER,¹ AND LUKAS NOVOTNY^{1,6}

¹Photonics Laboratory, ETH Zürich, Zürich, Switzerland

²Currently with the Department of Physics, Humboldt-Universität zu Berlin, 10099 Berlin, Germany

³Gaithersburg, MD 20877, USA

⁴Institute of Photonics, University of Eastern Finland, P.O. Box 111, FI- 80101 Joensuu, Finland

⁵Laboratoire Kastler Brossel, École Normale Supérieure-Université PSL, CNRS, Sorbonne Université, Collège de France, Paris 75005, France

⁶Quantum Center, ETH Zürich, Zürich, Switzerland

*anardi@ethz.ch

This supplement published with Optica Publishing Group on 23 November 2021 by The Authors under the terms of the [Creative Commons Attribution 4.0 License](https://creativecommons.org/licenses/by/4.0/) in the format provided by the authors and unedited. Further distribution of this work must maintain attribution to the author(s) and the published article's title, journal citation, and DOI.

Supplement DOI: <https://doi.org/10.6084/m9.figshare.17011997>

Parent Article DOI: <https://doi.org/10.1364/OE.442330>

Controlling spatial coherence with an optical complex medium: supplemental document

1. TECHNICAL LIMITATIONS

In the main text, we show that we encounter deviations between the encoded and the reconstructed degree of coherence when we try to achieve very low (approaching 0) or very high (approaching 1) values. In this section, we provide more details on the origins of these limits.

Let us start investigating the case where we want to obtain mutually incoherent outputs. According to Eq. (7) in the main text, the linear transformation we want to apply is the identity matrix, i.e., the inputs should be transmitted to the outputs unaffected. However, since it is not feasible to control all the modes supported by the scattering medium, the beams get mixed during the propagation through the medium. The resulting background noise is responsible for an unwanted contribution of each input field to every output.

We will now quantify the limitations to the minimum degree of coherence imposed by the background noise. We start considering a coherence matrix \mathbb{K}_{out} of the form

$$\mathbb{K}_{\text{out}} = \begin{bmatrix} 1 & \gamma & \cdots & \gamma \\ \gamma & 1 & \cdots & \gamma \\ \vdots & \ddots & \ddots & \vdots \\ \gamma & \gamma & \cdots & 1 \end{bmatrix}, \quad (\text{S1})$$

where, for simplicity, we set the off-diagonal terms to have the same constant real value γ . To have mutually incoherent output fields, we want γ to tend to 0. From \mathbb{K}_{out} we extract the expression of the linear transformation \hat{T} [Eq. (7) in the main text], which connects the mutually incoherent input fields E_{in} to the output fields E_{out} with coherence matrix \mathbb{K}_{out} . From the form we chose for \mathbb{K}_{out} [Eq. (S1)], the linear transformation \hat{T} can be completely described by two coefficients: t_{11} for the diagonal terms, which are all equal, and t_{21} for the off-diagonal elements, which are again all equal. Note that the coefficients t_{11} and t_{21} associate the two outputs E_1^{out} and E_2^{out} with the single input E_1^{in} , according to the relations $E_1^{\text{out}} = t_{11}E_1^{\text{in}}$, and $E_2^{\text{out}} = t_{21}E_1^{\text{in}}$ [Eq. (8) in the main text]. Ideally, we would like $|t_{21}|$ to approach zero to get zero output degree of coherence, i.e., we want $|E_2^{\text{out}}| = 0$. In practice, the background noise in the output intensity pattern poses a lower bound to the intensity $|E_2^{\text{out}}|^2$, hence to $|t_{21}|$, which finally sets the minimum degree of coherence different from zero. In Fig. S1a, we show the scaling of the absolute value of the ratio $|t_{21}|/|t_{11}|$ as a function of the degree of coherence γ . If we increase the number of inputs, i.e., the dimensionality of \mathbb{K}_{out} , the requirement is very similar (Fig. S1). A desired minimum degree of coherence translates into a minimum signal-to-noise ratio (SNR). In fact, considering the single input E_1^{in} and assuming that the only contribution to E_2^{out} is given by the background noise, $|t_{11}|^2$ is the maximum generated intensity and $|t_{21}|^2$ is the noise intensity, thus the SNR is defined as $|t_{11}|^2/|t_{21}|^2$. In Fig. S1b, we show that low coherence values demand very high SNR, which is limited by the number of SLM pixels modulating each input laser [1]. A similar argument works for a different form of \mathbb{K}_{out} , where the limitation is given by the element of the transformation \hat{T} with the minimum absolute value.

Let us now consider the factors limiting the maximum degree of coherence. To investigate this case, we turn on a single input (E_1^{in}), and we consider a single pair of output fields E_1^{out} and E_2^{out} , which are related to the input by the coefficients t_{11} and t_{21} , as discussed above. We compute the mutual degree of coherence

$$\gamma = \frac{\langle E_1^{\text{out}} (E_2^{\text{out}})^* \rangle}{\sqrt{\langle |E_1^{\text{out}}|^2 \rangle \langle |E_2^{\text{out}}|^2 \rangle}} = \frac{t_{11}t_{21}^* \langle |E_1^{\text{in}}|^2 \rangle}{|t_{11}t_{21}| \langle |E_1^{\text{in}}|^2 \rangle} = \frac{t_{11}t_{21}^*}{|t_{11}t_{21}|}, \quad (\text{S2})$$

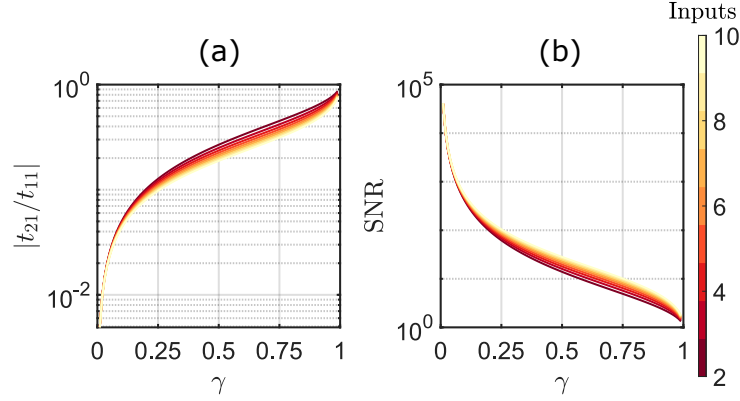


Fig. S1. Minimum degree of coherence limitations. (a) Given two outputs $E_1^{\text{out}} = t_{11}E_1^{\text{in}}$ and $E_2^{\text{out}} = t_{21}E_1^{\text{in}}$, the degree of coherence γ depends on the ratio $|t_{21}/t_{11}|$. (b) Minimum signal-to-noise ratio (SNR) needed to encode the degree of coherence γ . In the case that $|t_{21}|$ is only given by the background noise, the SNR is $|t_{11}|^2/|t_{21}|^2$.

whose modulus $|\gamma|$ is always equal to 1, regardless the values of the transformation coefficients. Nevertheless, the measurements deviate from this ideal result. To show it, we use a single input laser to generate through our system two output beams. We then let the output beams interfere and we reconstruct the degree of coherence. We report the measured interference patterns for two different input lasers in Fig. S2a and S2b. The reconstructed degrees of coherence ($\gamma_1 = 0.86$ for the first input and $\gamma_1 = 0.92$ for the second) are lower than the ideal value of 1. This discrepancy, in line with what is reported in literature, is associated to the limited spatial coherence of the light source [2]. We show now that the maximum degree of coherence achievable with a single laser is limiting the value obtainable by the whole system. Let us consider two mutually incoherent inputs, both of them contributing to two output fields. Since the components from the different inputs do not interfere, the resulting interference pattern is given by the sum of the individual patterns. Thus, we can write the visibility in terms of the maximum $I_1^{\text{max}}, I_2^{\text{max}}$ and minimum $I_1^{\text{min}}, I_2^{\text{min}}$ intensity given by the contributions from the two different inputs:

$$\mathcal{V} = \frac{(I_1^{\text{max}} + I_2^{\text{max}}) - (I_1^{\text{min}} + I_2^{\text{min}})}{(I_1^{\text{max}} + I_2^{\text{max}}) + (I_1^{\text{min}} + I_2^{\text{min}})}. \quad (\text{S3})$$

After few algebraic passages, we get

$$\mathcal{V} = \frac{\mathcal{V}_1}{1 + \frac{(I_2^{\text{max}} + I_2^{\text{min}})}{(I_1^{\text{max}} + I_1^{\text{min}})}} + \frac{\mathcal{V}_2}{1 + \frac{(I_1^{\text{max}} + I_1^{\text{min}})}{(I_2^{\text{max}} + I_2^{\text{min}})}}, \quad (\text{S4})$$

where $\mathcal{V}_i = (I_i^{\text{max}} - I_i^{\text{min}})/(I_i^{\text{max}} + I_i^{\text{min}})$ is the visibility of the interference pattern given by the i th input. Considering $I_1^{\text{max}} = I_2^{\text{max}}$ and $I_{1,2}^{\text{max}} \gg I_{1,2}^{\text{min}}$, we obtain

$$\mathcal{V} \approx \frac{\mathcal{V}_1 + \mathcal{V}_2}{2}. \quad (\text{S5})$$

The last equation tells us that the maximum visibility obtainable by the whole system [directly linked to the degree of coherence, see Eq. (11a) in the main text] is limited by the average visibility over each single input. Therefore, the maximum degree of coherence achievable is limited by the spatial coherence of the light sources. Figure S2 shows the interference pattern when we turn on: (a) only the first input, (b) only the second one, or (c) both of them. The measured degrees of coherence resulting from the combination of the two inputs ($\gamma_{12} = 0.89$) is in agreement with Eq. (S5).

2. MUTUAL INCOHERENCE OF THE INPUT FIELDS

Our implementation relies on mutually incoherent inputs. To achieve this condition, we used three red lasers (Thorlabs HRP050 and Meredith Instruments 633 nm HeNe lasers, and ≈ 650 nm

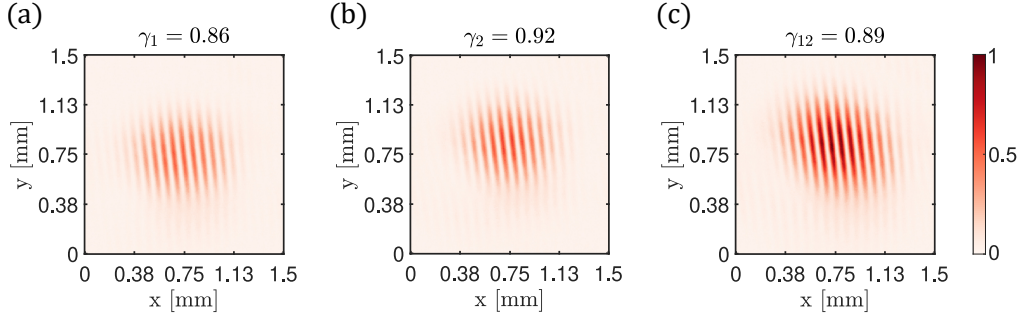


Fig. S2. Interference patterns. We have two interfering output fields, resulting from the superposition of two inputs. We show the interference patterns when (a) the first, (b) the second or (c) both inputs contribute to the outputs. Each case is associated to a measured degree of coherence γ_i , where the subscript i indicates the contributing inputs.

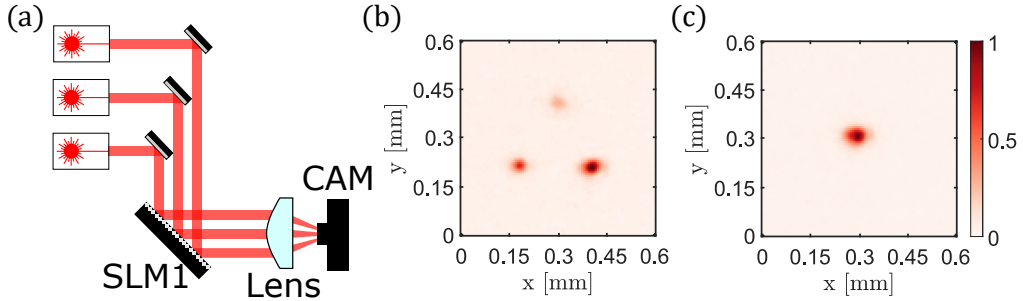


Fig. S3. Mutually incoherent inputs. (a) Characterization setup. Three independent laser beams are modulated by a SLM before being focused onto a camera. (b, c) Camera images. The SLM is used to (b) separate the beams in the focal plane or to (c) focus them in the same point. No interference fringes are present when the beams overlap, confirming that the three fields are mutually incoherent.

pen-type visual fault locator FOSCO BOB-VFL650-10), with a linewidth (HeNe ≈ 10 MHz, VFL ≈ 1 THz) much larger than the bandwidth of the employed detector (Basler acA640-750um, bandwidth $\approx 10 \div 100$ Hz). This ensures that we can consider them mutually incoherent. To confirm it, we focused the three laser beams into a single spot, checking that no interference fringes are visible (see Fig. S3).

3. COHERENCE MATRIX SPACE

In this section we describe the space of the allowed coherence matrices. As discussed in the main text, the coherence matrix is Hermitian and normalized such that its diagonal elements are 1. For three field E_1 , E_2 and E_3 , these conditions leave three degrees of freedom, which are the mutual degrees of coherence γ_{12} , γ_{13} and γ_{23} . Even though the degrees of coherence are complex quantities, in this work we focus specifically on their magnitudes, as the phase corresponds only to a spatial shift of the interference fringes. Thus, for three fields, we can visualize all possible combinations of the degree of coherence magnitudes in a three-dimensional space. However, not any combination of degrees of coherence is physically acceptable. In fact, the coherence matrix must also be positive semi-definite [3]. It translates into the condition of real and positive (or zero) eigenvalues. We show in Fig. S4 the contour of the space where the positive semi-definiteness is satisfied.

4. LINEAR PORT

In this section we characterize the linear transformation implemented with the system of complex medium and SLM. In the main text, we focused on the specific case of a 3×3 -port, that is a device that mixes three input fields into three output fields with controlled amplitude and phase. Thus, each input E_i^{in} generates three outputs according to $E_1^{\text{out}} = t_{1i}E_i^{\text{in}}$, $E_2^{\text{out}} = t_{2i}E_i^{\text{in}}$ and

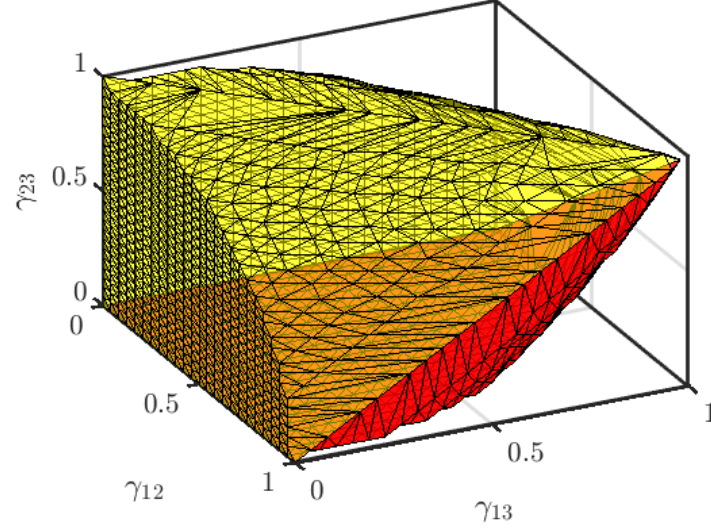


Fig. S4. Graphical representation of the space of allowed coherence matrices for three fields E_1 , E_2 and E_3 . γ_{ij} represents the magnitude of the mutual degree of coherence of the two fields E_i and E_j .

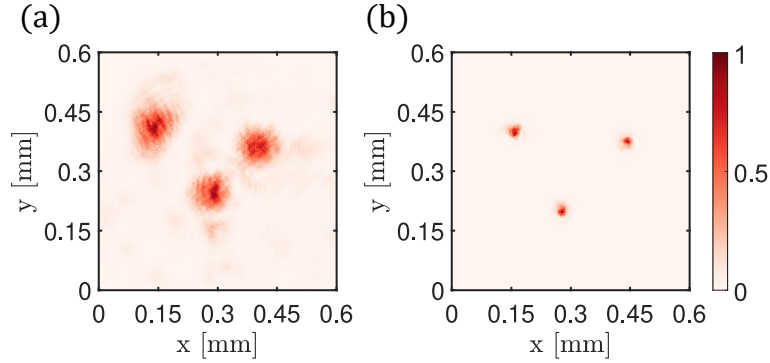


Fig. S5. Spatial filtering. Output fields' intensity distributions (a) before and (b) after three small circular apertures placed before the second SLM.

$E_3^{\text{out}} = t_{3i}E_i^{\text{in}}$. Turning off two of the three inputs, we can experimentally measure the coefficients t_{1i} , t_{2i} and t_{3i} . Characterizing these coefficients is the topic of the present section.

We consider the input E_1^{in} , and we measure the output intensities $I_1 = |t_{11}E_1^{\text{in}}|^2$, $I_2 = |t_{21}E_1^{\text{in}}|^2$ and $I_3 = |t_{31}E_1^{\text{in}}|^2$. We show an example of the resulting intensity distributions in Fig. S5a. The output beams, resulting from a speckle pattern, do not show a clean Gaussian profile. This is detrimental for the reconstruction of the degree of coherence from the interference pattern. Therefore, we introduce three small circular apertures (0.5 mm in diameter, spaced by roughly 2 mm) before the second SLM. We show in Fig. S5b the resulting spatially filtered beams.

We then characterize the output intensities when we modify the encoded coefficients. Given the desired coefficients, we calculate the needed SLM mask $\hat{t}_{\text{SLM},i}$ according to Eq. (10) in the main text. We then increase the magnitudes of t_{21} and t_{31} from 0 to 1, keeping t_{11} constant and equal to 1 (Fig. S6a). We measure that I_1 decreases while we increase the intensities I_2 and I_3 . This happens mainly because the overall power distributed in the three outputs is conserved between the transformations. Thus, if we increase the intensities of the second and third output, then I_1 must decrease accordingly. We correct for this effect by characterizing the intensity ratios I_2/I_1 and I_3/I_1 , which are the relevant quantities for the linear port (Fig. S6b), and we use the measured characteristics to calibrate the SLM masks. We repeat the measurement 100 times (for a total time of about 30 minutes), resulting in the reported error bars, which show the maximum

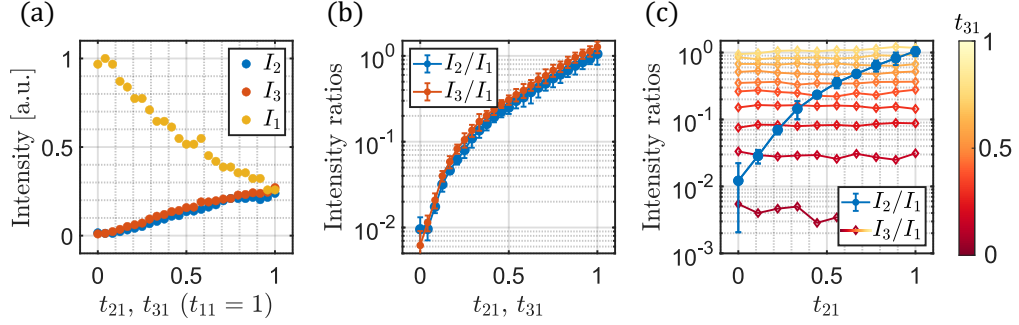


Fig. S6. Linear port characterization. (a) Power conservation. If we increase t_{21} and t_{31} , keeping constant t_{11} , the amplitude of the high intensity output reduces, to conserve the overall power shared between the outputs. (b) Intensity ratios. We measured the ratios I_2/I_1 and I_3/I_1 for increasing t_{21} and t_{31} . The error bars (which show the maximum deviation from the mean value) are obtained repeating the measurement 100 times. (c) Cross-talk analysis. We modulate t_{21} from 0 to 1, while keeping t_{31} constant. We repeat the measurement changing the value of t_{31} . The error bars on I_2/I_1 show the maximum deviation from the mean value.

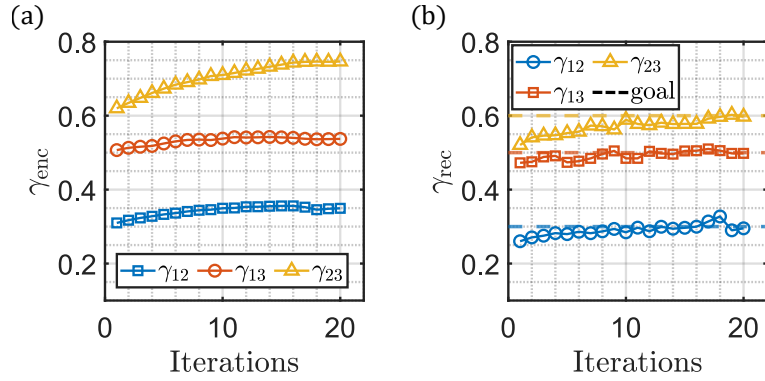


Fig. S7. Feedback. (a) The encoded values γ_{enc} are iteratively corrected using the error between the desired and the measured degrees of coherence. (b) Consequently, the reconstructed degrees of coherence γ_{rec} converge to the desired values, which in this case are $\gamma_{12} = 0.3$, $\gamma_{13} = 0.5$ and $\gamma_{23} = 0.6$.

deviation from the mean value.

The next step is to characterize the cross-talk between the output beams. In fact, if the outputs are not completely independent, changing the intensity of one of them will affect the other two. In Fig. S6c we increase the intensity of the output I_2 (t_{21} from 0 to 1), while keeping I_3 constant. We then repeat the measurement increasing the magnitude of t_{31} . We find that the fluctuations of the intensity I_3 are within the error bar of I_2 , which is comparable to the typical error that we report in Fig. S6b. We then conclude that the systematic cross-talk is below the statistical noise, hence not relevant.

5. GRADIENT DESCENT OPTIMIZATION

In this section we describe the feedback mechanism employed to achieve the accuracy in the control of the coherence matrix reported in the main text. Mainly due to errors in the calibration of the SLM phase masks [$\hat{T}_{\text{SLM},i}$ in Eq. (10) of the main text], we measure deviations between the reconstructed and the encoded degrees of coherence. Thus, we use a gradient descent algorithm to minimize the encoding errors.

Let us consider the pair of fields E_i and E_j . At the n th iteration step, we encode the degree of coherence $\gamma_{ij}^{\text{enc}}(n)$, and reconstruct $\gamma_{ij}^{\text{rec}}(n)$. We evaluate the encoding error $\epsilon(n) = \gamma_{ij}^{\text{rec}}(n) - \gamma_{ij}^{\text{enc}}(n)$ and, for the next iteration, we correct the encoded value following the relation

$$\gamma_{ij}^{\text{enc}}(n+1) = \gamma_{ij}^{\text{enc}}(n) + \eta \epsilon(n), \quad (\text{S6})$$

where η is the feedback strength, that we used for all the coherence matrices. From the new values of $\gamma_{ij}^{\text{enc}}(n+1)$ for each pair, we construct the corrected linear port. We reiterate the process until we are satisfied with the final encoding error ($\varepsilon < 0.01$ in our case). The gradient descent is the last step of the calibration of the setup. After running it once, we know the coefficients of the linear port which minimize the error, and the reconstructed degree of coherence is stable over time.

We illustrate the optimization procedure in Fig. S7. We want to encode the values $\gamma_{12} = 0.3$, $\gamma_{13} = 0.5$ and $\gamma_{23} = 0.6$. At each iteration, we correct the encoded values (Fig. S7a), while the reconstructed degree of coherence converge to the desired quantity (Fig. S7b).

6. UNITARITY OF A LINEAR TRANSFORMATION AND OVERALL COHERENCE

Let us consider a set of normalized input fields E_{in} , characterized by a coherence matrix $\mathbb{K}_{\text{in}} = \langle E_{\text{in}} E_{\text{in}}^\dagger \rangle$. We apply a unitary transformation \hat{U} to get the set of output fields $E_{\text{out}} = \hat{U} E_{\text{in}}$, with coherence matrix $\mathbb{K}_{\text{out}} = \langle E_{\text{out}} E_{\text{out}}^\dagger \rangle$. By definition, the unitary transformation \hat{U} satisfies the relation $\hat{U} \hat{U}^\dagger = \hat{U}^\dagger \hat{U} = \mathbb{I}$, where the symbol \dagger stands for the conjugate transpose, and \mathbb{I} is the identity matrix.

The overall coherence \mathcal{S} of the system of n fields E_{out} is defined as [4]

$$\mathcal{S} = \frac{n}{n-1} \left[\frac{\text{tr}(\mathbb{K}_{\text{out}}^2)}{(\text{tr} \mathbb{K}_{\text{out}})^2} - \frac{1}{n} \right], \quad (\text{S7})$$

where tr stands for matrix trace. This quantity is invariant under unitary transformation. To prove it, we expand the traces

$$\text{tr}(\mathbb{K}_{\text{out}}^2) = \text{tr}(\langle E_{\text{out}} E_{\text{out}}^\dagger \rangle^2) = \text{tr} \left[\left(\hat{U} \langle E_{\text{in}} E_{\text{in}}^\dagger \rangle \hat{U}^\dagger \right)^2 \right] = \text{tr} \left[\left(\hat{U} \mathbb{K}_{\text{in}} \hat{U}^\dagger \right)^2 \right], \quad (\text{S8})$$

$$\text{tr}(\mathbb{K}_{\text{out}}) = \text{tr}(\langle E_{\text{out}} E_{\text{out}}^\dagger \rangle) = \text{tr} \left[\hat{U} \langle E_{\text{in}} E_{\text{in}}^\dagger \rangle \hat{U}^\dagger \right] = \text{tr} \left[\hat{U} \mathbb{K}_{\text{in}} \hat{U}^\dagger \right], \quad (\text{S9})$$

and, using the definition of unitary transformation and the cyclic property of the trace, we obtain

$$\text{tr}(\mathbb{K}_{\text{out}}^2) = \text{tr}(\hat{U} \mathbb{K}_{\text{in}} \hat{U}^\dagger \hat{U} \mathbb{K}_{\text{in}} \hat{U}^\dagger) = \text{tr}(\mathbb{K}_{\text{in}} \hat{U}^\dagger \hat{U} \mathbb{K}_{\text{in}} \hat{U}^\dagger \hat{U}) = \text{tr}(\mathbb{K}_{\text{in}}^2). \quad (\text{S10})$$

$$\text{tr}(\mathbb{K}_{\text{out}}) = \text{tr}(\hat{U} \mathbb{K}_{\text{in}} \hat{U}^\dagger) = \text{tr}(\mathbb{K}_{\text{in}} \hat{U}^\dagger \hat{U}) = \text{tr}(\mathbb{K}_{\text{in}}). \quad (\text{S11})$$

We proved that $\text{tr}(\mathbb{K}_{\text{out}}^2) = \text{tr}(\mathbb{K}_{\text{in}}^2)$ and $\text{tr}(\mathbb{K}_{\text{out}}) = \text{tr}(\mathbb{K}_{\text{in}})$, thus confirming that the overall coherence remains unaffected under unitary transformations.

REFERENCES

1. S. M. Popoff, G. Lerosey, M. Fink, A. C. Boccarda, and S. Gigan, "Controlling light through optical disordered media: Transmission matrix approach," *New J. Phys.* **13**, 123021 (2011).
2. L.-P. Leppänen, K. Saastamoinen, A. T. Friberg, and T. Setälä, "Measurement of the degree of temporal coherence of unpolarized light beams," *Photon. Res.* **5**, 156–161 (2017).
3. L. Devroye, *Non-Uniform Random Variate Generation* (Springer, 1986).
4. J. J. Gil, "Sources of asymmetry and the concept of nonregularity of n-dimensional density matrices," *Symmetry* **12**, 1002 (2020).